Seismic Behaviour and Strengthening of Rammed Earth Constructions

D. V. Oliveira(✉), A. Romanazzi, R. A. Silva, A. Barontini, and N. Mendes

University of Minho, ISISE, Guimarães, Portugal
danvco@civil.uminho.pt

Abstract. The widespread use of earthen buildings can be accredited to the local availability of the raw material, sustainability of the building process, and low cost. Earthen structures suffer from high seismic vulnerability, resulting from the low strength of the material, high mass, and lack of engineering approaches in design and building. Despite the extensive use of rammed earth structures, the structural behaviour of such buildings is still not well known, particularly concerning the in-plane and out-of-plane response under cyclic loads. Moreover, proper strengthening solutions are still required to reduce seismic vulnerability. In this context, an experimental program was conducted on the in-plane and out-of-plane cyclic performance of rammed earth structural sub-assemblies. The prototypes, after being damaged, were strengthened by employing a TRM-based solution and subjected to further testing. The experimental results are reported and discussed in terms of cracking pattern and peak base shear coefficient. Finally, the effectiveness of the proposed strengthening solution was evaluated against the performance of the unstrengthened mockups. The outcomes highlighted the effectiveness of the TRM solution in improving the ductility and the in-plane shear capacity of the mockups.

Keywords: Rammed earth · in-plane test · shaking table test · compatible strengthening · textile-reinforced mortar

1 Introduction

Earthen materials have been extensively observed as part of architectural heritage of various civilizations, including religious and civil monuments, entire historical towns and archaeological sites. In addition, about one-fourth of the global population is estimated to live in earthen buildings [1–3]. The historic popularity of earthen materials can derive from the local availability of the raw material, sustainability of the process, ease of building, adequate thermal and acoustic isolation, and low cost. Consequently, several building techniques based on the use of soil were developed, yet adobe, compressed earth blocks and rammed earth are among the most used nowadays. On the other hand, earth architecture is characterised by high seismic vulnerability, which results from low to moderate strength of the material, poor structural maintenance and lack of engineering approach in design and building practices. In this context, the need to protect cultural heritage while containing casualties remarks the importance of finding appropriate

Y. Endo and T. Hanazato (Eds.): SAHC 2023, RILEM Bookseries 47, pp. 1214–1225, 2024.
https://doi.org/10.1007/978-3-031-39603-8_98

strengthening solutions to reduce the seismic vulnerability of earthen structures [4–6]. In response, the research on strengthening systems for rammed earth is rather recent and the strengthening with textile reinforced mortar (TRM) needs further research for its application on rammed earth structures [7–10]. In addition, the response of unstrengthened rammed earth structures is still not well known, in particular with regard to the in-plane and out-of-plane behaviour of the walls under cyclic and dynamic excitation. Given the above framework, to evaluate the performance of the unstrengthened rammed earth structure and the effectiveness of a TRM-strengthening solution proposed, the main outcomes of quasi static cyclic in-plane and dynamic out-of-plane tests on rammed earth sub-assemblies are here presented and discussed.

2 Quasi-static In-Plane Cyclic Test

2.1 Experimental Setup

In order to assess the in-plane response of rammed earth walls of traditional single-storey buildings with timber roof, a reduced scale 1:1.25 sub-assembly was built with an I-shape geometry plan. The geometry was defined based on a preliminary numerical investigation [11]. In addition, to simulate a traditional timber roof, the wall was loaded for a total weight of 11.77 kN after a drying period of four months. The test setup was designed to allow the application of cyclic horizontal displacements at the top and it was conducted by controlling the displacement in the loading direction of a point at the top of the left wing (control point) (see Fig. 1a). The cyclic testing protocol considered increasing the target displacements in both directions (positive and negative), and one repetition for each positive and negative cycle. The displacements were recorded by a set of LVDTs set along the vertical profile of the mockup, as illustrated in Fig. 1b. Further details on the materials, construction, and test setup can be found in [12, 13].

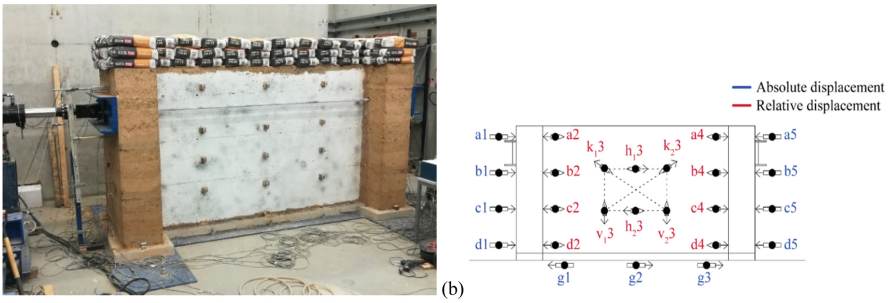

Fig. 1. In-plane cyclic test: a) mockup; b) LVDTs setup.

2.2 Results and Discussion of the Unstrengthened Mockup

The results of the in-plane cyclic test for the unstrengthened rammed earth model (URE-IP) are hereinafter presented and discussed in terms of cracking pattern and base shear

coefficient (BSC). Minor cracks were first observed on wing-walls close to the loading surface, however, a main horizontal crack formed in the web-wall along one of the interfaces between layers. Afterwards, further two diagonal cracks opened at the lower inner corner of the web-wall, connecting with the previous horizontal crack, as shown in Fig. 2. Based on this observation, the URE-IP wall responded as a non-homogeneous material as a consequence of the low tensile and shear strength of the interface between layers and low vertical loads.

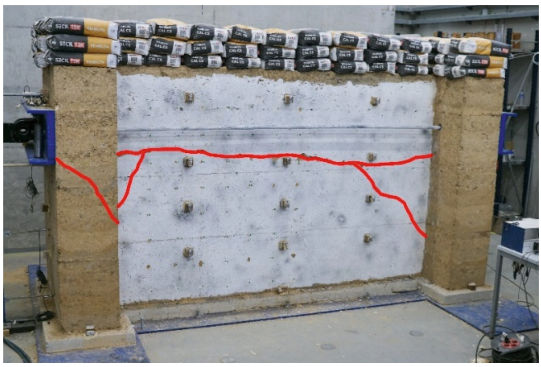

Fig. 2. Crack pattern of URE-IP model.

The BSC curves are illustrated in Fig. 3a. The peak BSC in the positive direction was 1.18 and was achieved for a displacement of 0.90 mm during the fourth cycle. While the peak BSC toward the negative direction was 1.39 and was reached with a displacement of 2.70 mm. The envelope of the BSC shows clearly a linear response followed by a non-linear behaviour due to the opening of the cracks, and the subsequent softening response suggests friction at the interface of the main horizontal crack (see Fig. 3b).

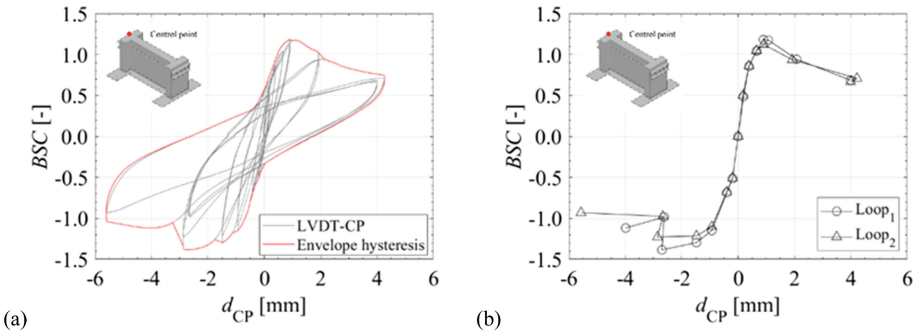

Fig. 3. Results of URE-IP model: a) overall curves; b) envelope curve of loops.

2.3 Results and Discussion of TRM-Strengthened Mockup

After testing, the unstrengthened rammed earth wall was strengthened with a compatible TRM solution based on a geo-mesh (GeoRE-IP), which was embedded in a layer of earth-based mortar (see Fig. 4). As for the URE-IP case, the cyclic testing protocol considered increasing target displacements in both loading directions, and two loops for each cycle, see also [12]. Following, the results of the in-plane cyclic test for the GeoRE-IP model are discussed and compared with those of the URE-IP model, in terms of cracking pattern and base shear coefficient. The GeoRE-IP model showed at first minor cracks in correspondence with the main crack of the previous URE-IP model, which progressively developed with the consequent detachment of the mortar. At the final stage, further diagonal cracks opened, while another horizontal crack formed at the top zone of the web-wall, see Fig. 5. In general, the overall cracking pattern indicated that the damaged state of the previous unstrengthened structure was difficult to be recovered; however, the TRM strengthening was effective in redistributing the loads to the entire structure, as demonstrated by the opening of new cracks.

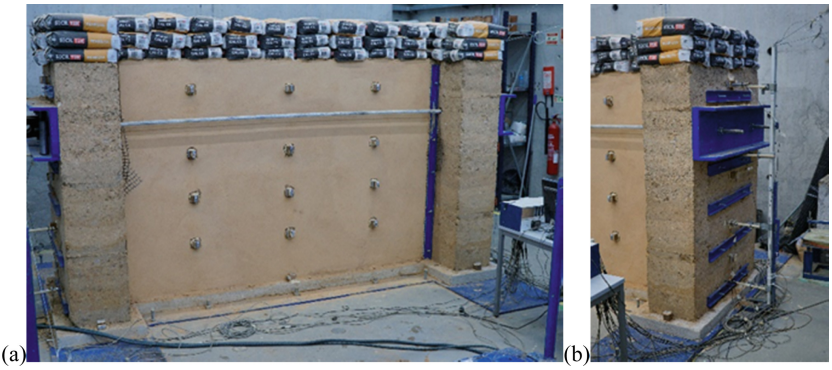

Fig. 4. TRM-strengthening system: a) web-wall; b) wing-wall.

To assess the effectiveness of the TRM-strengthening and for the sake of brevity, Fig. 6a reports the comparison between the BSC envelope curves of the GeoRE-IP and URE-IP tests. The GeoRE-IP model attained a BSC peak towards the positive direction of 1.23 and achieved a displacement of 6.67 mm. While the peak BSC towards the negative direction was 1.29 and was reached with a displacement of 9.15 mm. The comparison between GeoRE-IP and URE-IP models showed that the strengthened rammed earth model was characterised by an early nonlinear response, which confirmed that the previous damage state could not be recovered by the TRM-strengthening (Fig. 6b). Nevertheless, the GeoRE-IP presented a gain of 4% in shear strength capacity that was attained with a drift increase of 600% with respect to the unstrengthened model URE-IP; whereas in the case of the loading in the negative direction, the strengthened model could recover up to 93%, however, the peak was achieved with an increment of 235% in drift.

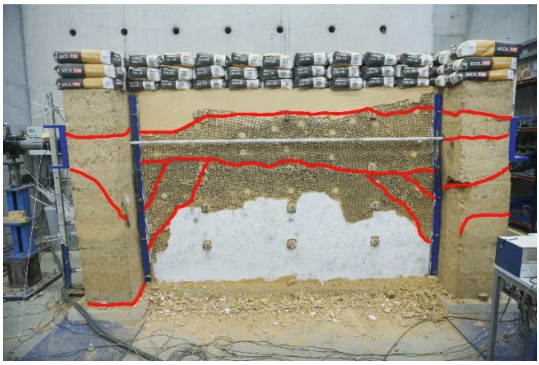

Fig. 5. Crack pattern of GeoRE-IP model.

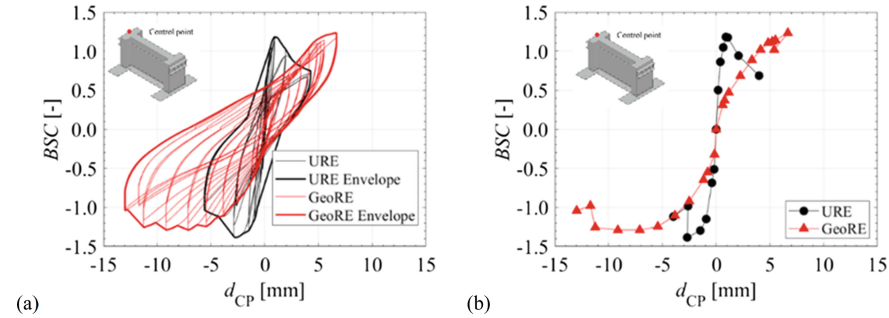

Fig. 6. Comparison between GeoRE-IP and URE-IP models: a) overall curves; b) envelope curves.

3 Out-Of-Plane Shaking Table Test

3.1 Experimental Setup

The geometry of the mockup was defined to simulate the out-of-plane behaviour of a rammed earth wall, which is found to be one of the most common collapse mechanisms [14–17]. Thus, the rammed earth sub-assembly was built with a U-shape plan with the dimensions as illustrated in Fig. 7. It is worth noting that such geometry is representative of the geometry of sub-assemblies found in vernacular rammed earth constructions from Alentejo [2, 3, 18].

The seismic tests were performed in the Earthquake Engineering and Structural Dynamics Division (NESDE) at the National Laboratory of Civil Engineering (LNEC), in Lisbon. The generated time histories were based on stochastic methods and on a seismological model that considers finite fault effects [19] and were amplified through increasing scale factors at each step of the experimental program. The seismic tests on the unstrengthened URE-ST mockup were performed until attaining a damage level that would not compromise its structural equilibrium. Further details on the materials, construction and test setup can be found in [12, 20]. To represent each seismic signal,

the peak ground parameters (PGA, PGV and PGD) were selected. To monitor the out-of-plane response of the mockup, 6 accelerometers were set on the West façade (AW01 to AW06) (Fig. 8a), while 15 accelerometers (AE01 to AE15) were placed on the East side of the core-wall and wing walls ((Fig. 8c). Further 4 accelerometers were placed on the South façade (AS01 and AS02) and the North façade (AN01 and AN02), see Fig. 8b and Fig. 8d.

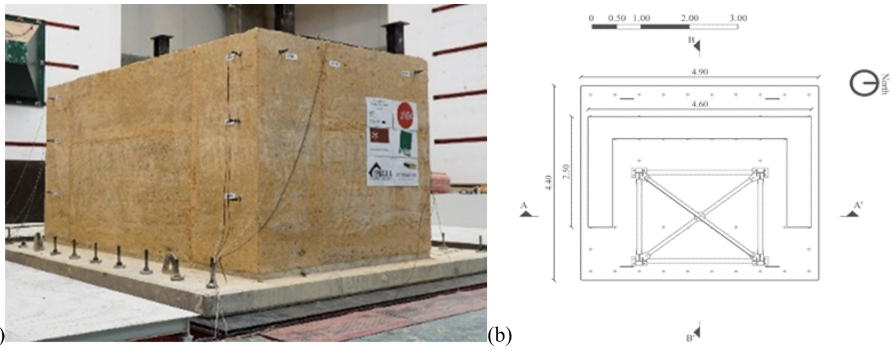

Fig. 7. Out-of-plane shaking table test: a) mockup, and b) geometry.

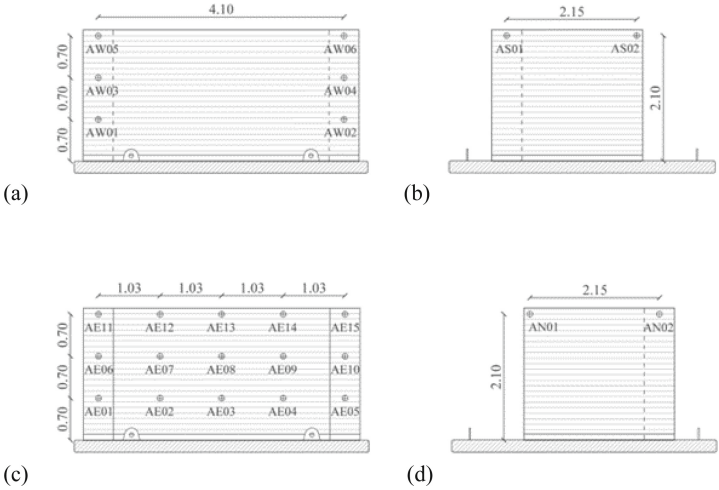

Fig. 8. Setup of the accelerometers of the shaking table test: a) West façade; b) South façade; c) East façade; d) North façade.

3.2 Results and Discussion of the Unstrengthened Mockup (URE-ST)

The results of the shaking table tests on the unstrengthened mockup URE-ST are hereinafter presented in terms of cracking pattern, displacements and base shear coefficient.

A horizontal crack could only be observed at the last seismic input, and it was located at an interface between two layers of rammed earth in lower sections of the wing-walls (Fig. 9). Such cracking pattern highlighted the lower tensile strength of the interface between two rammed earth layers, as also reported in the in-plane cyclic tests (see Sect. 2.2).

The displacements attained by the unstrengthened mockup were calculated from the accelerations recorded by AE01 to AE15. Afterwards, the maximum displacement of the control point (CP) was considered to perform regression analysis with the peak ground parameters, as reported in (Fig. 10). As a result, quadratic and linear regressions with high correlation coefficients were found. Therefore, it was observed that the maximum out-of-plane displacement can be predicted with a high level of confidence based on the time history of the seismic event.

The base shear coefficient (BSC) developed during the seismic tests was evaluated by summing the inertial forces of a lumped mass model equivalent to the real structure [20]. Afterwards, regression analyses were performed in terms of the absolute maximum BSC, while considering the peak ground parameters as an independent variable. As a result, linear relationships with a high correlation coefficient were found between the maximum BSC and PGA and PGV (Fig. 11a and Fig. 11b). Nevertheless, no correlation was found between the PSD and the maximum absolute BSC (Fig. 11c), which might be a consequence of the natural period of the structure concerning the frequency content of the ground motion.

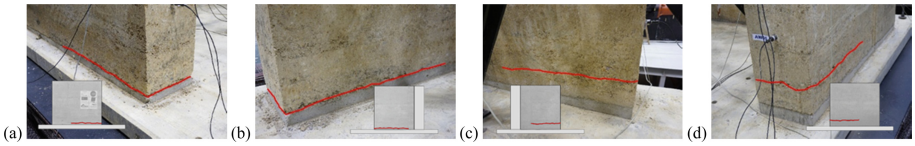

Fig. 9. Crack pattern of URE-ST: a) exterior South façade; b) interior South façade; c) interior North façade; d) exterior North façade.

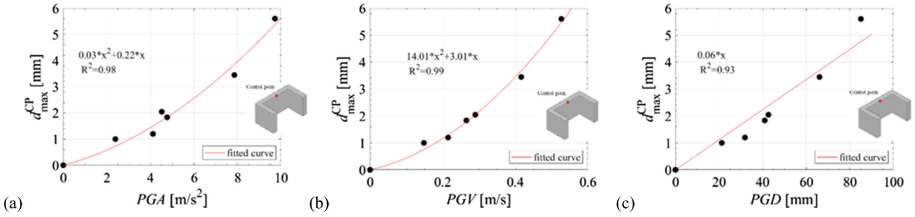

Fig. 10. Regression analysis between the maximum displacement of control point of URE-ST and: a) PGA; b) PGV; c) PGD.

3.3 Results and Discussion of TRM-Strengthened Mockup

After the series of seismic tests conducted on the URE-ST mockup, a TRM system was applied with the use of a nylon mesh embedded in a layer of earth-based mortar. The

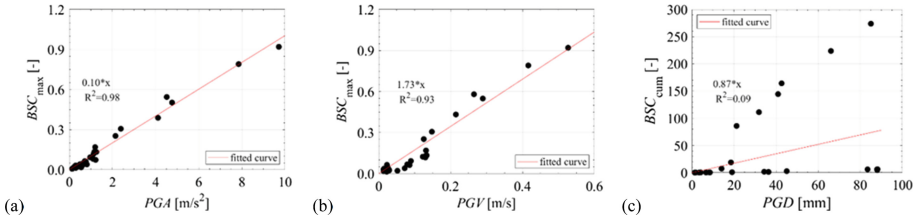

Fig. 11. Regression analysis between maximum BSC of URE-ST and: a) PGA; b) PGV; c) PGD.

experimental protocol of the strengthened mockup NRE-ST followed the same strategy considered in the previous URE-ST test. Further details can be found in [12]. The outcomes of the shaking table tests of the NRE-ST mockup are hereinafter presented and compared concerning the results of the URE-ST mockup in terms of cracking pattern, displacements and base shear coefficient. Figure 12 shows a comparison of the crack pattern between the unstrengthened URE-ST mockup (in blue) and the TRM-strengthened mockup NRE-ST mockup (in red). It is observed that the horizontal openings in NRE-ST occurred at the same location of the previous URE-ST cracks. This suggests that the NTRM-strengthening could not recover the previous damage state, as one could expect. Subsequently, a marked diagonal crack occurred in the middle of the web-wall, indicating the onset of an out-of-plane mechanism.

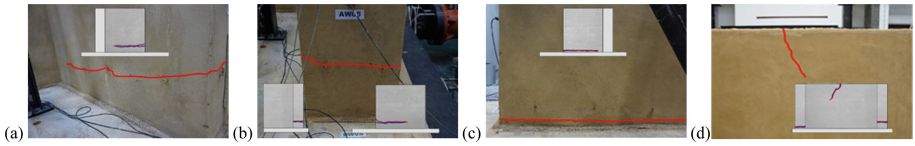

Fig. 12. Crack pattern of NRE-ST model: a) interior North façade, b) exterior North façade, c) interior South façade, and c) web-wall.

The displacements achieved by the NRE-ST mockup were assessed from the accelerations recorded by AE01 to AE15. Afterwards, regression analyses were performed in terms of the maximum displacements of the control point (CP) while considering the peak ground parameters. As a result, linear relationships with high correlation coefficients were found also in this case (Fig. 13). Therefore, the response in terms of maximum out-of-plane displacement of the wall can be predicted with high confidence based on the time history of the seismic event.

The effectiveness in terms of displacement capacity of the TRM solution demonstrates that the NRE-ST model attained an improvement of about 130% of the maximum displacement of the unstrengthened mockup (Fig. 14).

The base shear coefficient values BSC were here calculated as for the URE-ST model. Subsequently, regression analyses were conducted considering the absolute maximum BSC with the peak ground parameters. As a result, linear relationships with high correlation coefficients were found between the maximum BSC and PGA and PGV (Fig. 15a and Fig. 15b). Nevertheless, no correlation was found between the PGD and the maximum absolute BSC (Fig. 15d). As previously observed for the URE-ST mockup, such

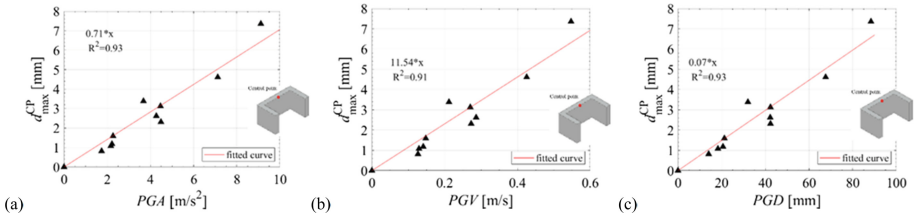

Fig. 13. Regression analysis between the maximum displacement of control point of NRE-ST and: a) PGA, b) PGV, and c) PGD.

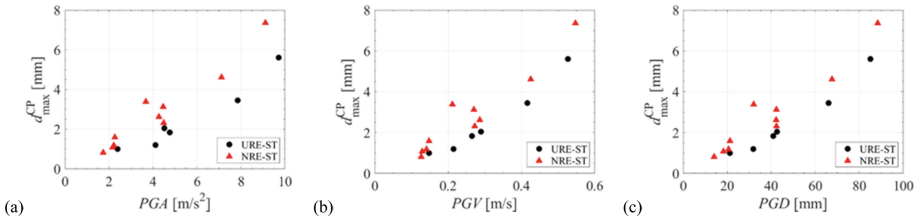

Fig. 14. Comparison of maximum displacement of control point between NRE-ST and URE-ST: a) PGA; b) PGV; c) PGD.

effect can be due to the natural period of the structure concerning the frequency content of the earthquake.

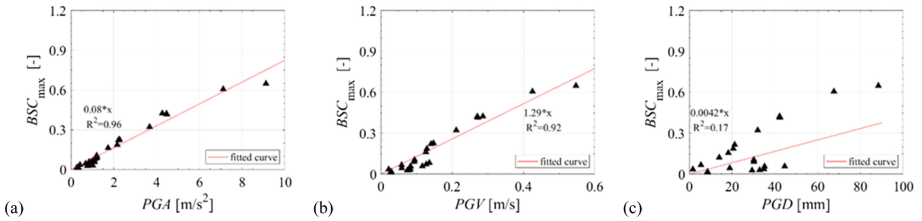

Fig. 15. Regression analysis between maximum BSC of NRE-ST and: a) PGA; b) PGV; c) PGD.

Afterwards, the effectiveness in terms of the capacity of the TRM solution showed that the capacity of the NRE-ST mockup was lower than the capacity attained by URE-ST (Fig. 16). Such results might indicate that the TRM-strengthening by embedding nylon mesh could not recover the existing structural damage and provide further strength when applied on a massive building subjected to dynamic loads.

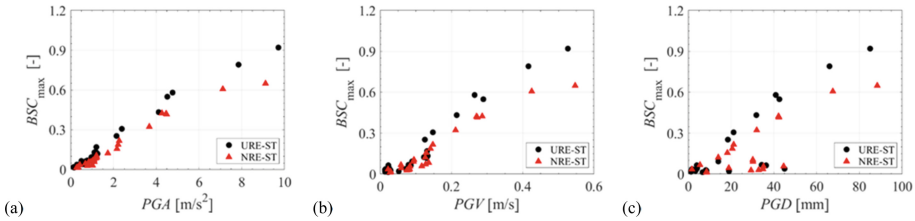

Fig. 16. Comparison of maximum BSC between NRE-ST and URE-ST: a) PGA; b) PGV; c) PGD.

4 Conclusion

The experimental program carried out intended to assess the hysteretic behaviour of rammed earth walls subjected to in-plane and out-of-plane excitations and evaluate the effectiveness of a novel TRM-strengthening solution.

As for the in-plane testing, the crack pattern of the URE-IP demonstrated that a rammed earth wall subjected to in-plane displacements cannot be assumed as a homogeneous material. Yet, the GeoRE-IP model cracking pattern indicated that the TRM-strengthening was able to redistribute the loads involving entirely the structure. Although the GeoRE-IP model showed an early nonlinear response consequent to the former damage state of the model, the TRM-strengthening resulted effective as it allowed achieving up to 104% of the BSC of the original structure for a drift increase of 600%. In conclusion, the adopted TRM-strengthening solution with the use of a geomesh was effective in recovering the strength capacity of the original structure while providing further dissipative and ductility capacities.

As for the out-of-plane dynamic response of the sub-assemblage, the cracking pattern of the URE-ST mockup confirmed the inferior tensile strength of the interfaces between rammed earth layers. The maximum out-of-plane displacement of the URE-ST mockup was found to be highly correlated with the peak ground parameters of the seismic inputs; meaning that the response in terms of maximum out-of-plane displacement may be predicted based on the ground motion. As well, the maximum BSC demonstrated linear relationships with a high coefficient of correlation with the ground motion parameters. The cracking pattern of the NRE-ST mockup suggested that the use of nylon mesh in the TRM-strengthening could not recover the previous damage state. Subsequently, linear and quadratic relationships with high coefficients of correlation were found for the maximum out-of-plane displacement of the NRE-ST as a function of the peak ground parameters characterising the seismic inputs. As well, linear relationships with a high coefficient of correlation were found to describe the maximum BSC of NRE-ST as a function of the ground motion parameters. Afterwards, the effectiveness of the TRM solution, evaluated by analysing the maximum base shear coefficient attained by the URE-ST and the NRE-ST mockups, reported that the URE-ST mockup presented a higher strength capacity, which suggested that the nylon mesh-based TRM-strengthening could not provide further strength when applied on such massive structure subjected to dynamic loads. In conclusion, the rammed earth sub-assemblage demonstrated sufficient out-of-plane capacity. However, the TRM-strengthening with the use of nylon mesh did

not provide further capacity to a massive structure under dynamic loads, for which a more resistant mesh, such as GeoM, would be probably required.

Acknowledgment. This work was partly financed by FEDER funds through the Operational Programme Competitiveness Factors (COMPETE 2020) and by national funds through the Foundation for Science and Technology (FCT) within the scope of project SafEarth—PTDC/ECM-EST/2777/2014 (POCI-01–0145-FEDER-016737). The support from grants SFRH/BD/131006/2017 and SFRH/BPD/97082/2013 is also acknowledged. Acknowledgments are addressed to the Laboratory of Structures (LEST) of the University of Minho, João Bernardino Lda and TERRACRUA Lda for building the rammed earth models.

References

1. Romanazzi, A., Oliveira, D.V., Silva, R.A.: Experimental investigation on the bond behavior of a compatible TRM-based solution for rammed earth heritage. Int. J. Archit. Herit. **13**(7), 1042–1060 (2019). https://doi.org/10.1080/15583058.2019.1619881
2. Silva, R.A., Mendes, N., Oliveira, D.V., Romanazzi, A., Domínguez-Martínez, O., Miranda, T.: Evaluating the seismic behaviour of rammed earth buildings from Portugal: from simple tools to advanced approaches. Eng. Struct. **157**, 144–156 (2018). https://doi.org/10.1016/j.engstruct.2017.12.021
3. Silva, R.A., Romanazzi, A., Oliveira, D.V., Domínguez-Martínez, O., Mendes, N.: Avaliação simplificada da vulnerabilidade sísmica de construções de taipa do Alentejo. Revista Portuguesa de Engenharia de Estruturas **3**(8), 59–70 (2018). https://repositorium.sdum.uminho.pt/bitstream/1822/67851/1/rpee_sIII_n08_pg59_70.pdf
4. Michiels, T.L.G.: Seismic retrofitting techniques for historic adobe buildings. Int. J. Archit. Herit. **9**(8), 1059–1068 (2015). https://doi.org/10.1080/15583058.2014.924604
5. Tolles, E.L.: Seismic studies on small-scale models on adobe houses. Blume Earthquake engineering Center (1990)
6. Tolles, E.L., Kimbro, E.E., Ginell, S.W.: Planning and engineering guidelines for the seismic retrofitting of historic adobe structures. Getty Publications (2002)
7. Romanazzi, A., Oliveira, D.V., and Silva, R.A. (2021) An analytical bond stress-slip model for a TRM composite compatible with rammed earth. Construction and Building Materials, 310. https://doi.org/10.1016/j.conbuildmat.2021.125228
8. Romanazzi, A., Van Gorp, M., Oliveira, D.V., Silva, R.A., Verstrynge, E.: Experimental shear behaviour of rammed earth strengthened with a TRM-based compatible technique. Key Eng. Mater. **817**, 544–551 (2019)
9. Romanazzi, A., Oliveira, D.V, Silva, R.A.: Experimental investigation on the bond behavior of a compatible TM-based solution for rammed earth heritage. Int. J. Archit. Herit. (2019). https://doi.org/10.1080/15583058.2019.1619881
10. Eudave, R.R., Silva, R.A., Pereira, E., Romanazzi, A.: Early-age shrinkage and bond of LC-TRM strengthening in rammed earth. Constr. Buildin Mat. 350 (2022). https://doi.org/10.1016/j.conbuildmat.2022.128809
11. Allahvirdizadeh, R., Oliveira, D.V., Silva, R.A.: Numerical investigation of the in-plane seismic performance of unstrengthened and TRM-strengthened rammed earth walls. Int. J. Archit. Herit. **15**(4), 548–566 (2021). https://doi.org/10.1080/15583058.2019.1629507
12. Romanazzi, A. (2022) Seismic protection of rammed earth heritage based on a compatible externally applied strengthening technique. Ph.D thesis, Universidade do Minho

13. Romanazzi, A., Oliveira, D.V., Silva, R.A., Barontini, A., Mendes, N.: Performance of rammed earth subjected to in-plane cyclic displacement. Mater. Struct. **55**(2), 1–17 (2022). https://doi.org/10.1617/s11527-022-01894-z
14. Barros, R.S., Costa, A., Varum, H., Rodrigues, H., Lourenço, P.B., Vasconcelos, G.: Seismic behaviour analysis and retrofitting of a row building. In Seismic Retrofitting: Learning from Vernacular Architecture, pp. 213–218 (2015). https://doi.org/10.1201/b18856-45
15. Bui, T.T., Bui, Q.B., Limam, A., Maximilien, S.: Failure of rammed earth walls: from observations to quantifications. Constr. Build. Mater. **51**, 295–302 (2014). https://doi.org/10.1016/j.conbuildmat.2013.10.053
16. Liu, K., Wang, M., Wang, Y.: Seismic retrofitting of rural rammed earth buildings using externally bonded fibers. Constr. Build. Mater. **100**, 91–101 (2015). https://doi.org/10.1016/j.conbuildmat.2015.09.048
17. Lourenço, P. B., Torrealva, D., Cancino, C., Wong, K., Karanikoloudis, G., & Ciocci, M. P. (2017). Innovative traditional technologies for rehabilitation and protection of earthen structures: the Getty conservation institute seismic retrofitting project. Proceeding of the 3rd International Conference on Protection of Historical Constructions, Lisbon, 12th - 15th July, 12–15
18. Allahvirdizadeh, R., Oliveira, D.V., Silva, R.A.: Numerical modeling of the seismic out-of-plane response of a plain and TRM-strengthened rammed earth subassembly. Eng. Struct. **193**, 43–56 (2019). https://doi.org/10.1016/j.engstruct.2019.05.022
19. Carvalho, A., Zonno, G., Franceschina, G., Serra, B., Campos Costa, A.: Earthquake shaking scenarios for the Metropolitan Area of Lisbon. Soil Dyn. Earthq. Eng. **28**, 347–364 (2008)
20. Romanazzi, A., Oliveira, D.V., Silva, R.A., Candeias, P.X., Costa, A.C., Carvalho, A.: Out-of-plane shaking table test of a rammed earth sub-assembly. Bull. Earthq. Eng. (2022). https://doi.org/10.1007/s10518-022-01525-6